

Tissue-Specific Expression of AHR2, ARNT2, and CYP1A in Zebrafish Embryos and Larvae: Effects of Developmental Stage and 2,3,7,8-Tetrachlorodibenzo-*p*-dioxin Exposure

Eric A. Andreasen,* Jan M. Spitsbergen,† Robert L. Tanguay,‡ John J. Stegeman,§
Warren Heideman,*¶ and Richard E. Peterson*¶¹

*Environmental Toxicology Center, University of Wisconsin, Madison, Wisconsin 53705; †Department of Environmental and Molecular Toxicology and Marine/Freshwater Biomedical Sciences Center, Oregon State University, Corvallis, Oregon 97333; ‡Department of Pharmaceutical Sciences, School of Pharmacy, University of Colorado Health Sciences Center, Denver, Colorado 80262; §Biology Department, Woods Hole Oceanographic Institute, Woods Hole, Massachusetts 02543; and ¶School of Pharmacy, University of Wisconsin, Madison, Wisconsin 53705

Received February 2, 2002; accepted April 10, 2002

To better understand the role of the aryl hydrocarbon receptor (AHR) signaling pathway in causing tissue-specific signs of 2,3,7,8-tetrachlorodibenzo-*p*-dioxin (TCDD) toxicity in zebrafish, the temporal and spatial expression of the zebrafish aryl hydrocarbon receptor 2 (*zfAHR2*), aryl hydrocarbon receptor nuclear translocator 2 (*zfARNT2*), and an AHR regulated gene, cytochrome P4501A (*zfCYP1A*), were assessed in larvae exposed to vehicle or TCDD (1.55 nM) from 3–4 h postfertilization (hpf). Coexpression of a transcriptionally active AHR pathway was apparent by the expression of *zfCYP1A* mRNA and protein in certain larval tissues. *zfCYP1A* protein was first detected in the skin and vasculature of TCDD-exposed larvae at 36 hpf. Vascular-specific *zfCYP1A* protein expression continued from 36 to 120 hpf at which time it was also detected in the heart, kidney, and liver. *zfCYP1A* mRNA was observed in TCDD treated larvae as early as 24 hpf in the developing vascular system. Vascular specific *zfCYP1A* mRNA expression in the head, trunk, and tail by 36 hpf in TCDD-exposed larvae, confirmed immunohistochemical localization. The expression of *zfAHR2* and *zfARNT2* mRNAs was generally similar in control and TCDD-exposed larvae. Coexpression of *zfAHR2*, *zfARNT2*, and *zfCYP1A* mRNAs was evident in TCDD-exposed larvae by 36 hpf and in the vasculature, heart, and trunk kidney by 48 hpf, well before the first signs of overt developmental toxicity are observed. In addition to their function in response to AHR agonists, *zfAHR2* and *zfARNT2* may be involved in development and function of the nervous system. *zfAHR2* and *zfARNT2* were detected in the brain, spinal cord, and sensory organs. However, TCDD-induced *zfCYP1A* expression was not detected in these tissues. Taken together, these results are consistent with the notion that the cardiovascular system is a primary target of TCDD developmental toxicity in zebrafish.

Key Words: AHR; ARNT; CYP1A; TCDD; zebrafish; embryo; larva; development; expression; toxicity.

Larval fish exposed to sufficiently high tissue concentrations of aryl hydrocarbon receptor (AHR) agonists such as the polychlorinated dibenzo-*p*-dioxins (PCDDs), dibenzofurans (PCDFs), and biphenyls (PCBs) exhibit similar signs of developmental toxicity. These signs include yolk sac, pericardial and meningeal edema, decreased cardiac output, reduced blood flow to most peripheral vascular beds, anemia, multifocal hemorrhage, impaired swimbladder inflation, craniofacial malformations typified by impaired lower jaw development, stunted growth, and mortality (Belair *et al.*, 2001; Elonen *et al.*, 1998; Henry *et al.*, 1997; Johnson *et al.*, 1998; Spitsbergen *et al.*, 1990; Teraoka *et al.*, 2002; Walker and Peterson, 1991; Walker *et al.*, 1991; Zabel *et al.*, 1995). Exposure of the most sensitive fish species to such AHR agonists is of ecological concern because of their potential to reduce feral fish populations secondary to mortality at the larval stage of development (Walker and Peterson, 1994; Zabel *et al.*, 1995).

Effort to understand the molecular mechanism of 2,3,7,8-tetrachlorodibenzo-*p*-dioxin (TCDD) developmental toxicity has led to the characterization of the AHR pathway in mammals and other model organisms including zebrafish. In mammals, much of the toxicity of TCDD-like AHR ligands is dependent upon their binding to the cytosolic AHR (Rowlands and Gustafsson, 1997; Schmidt and Bradfield, 1996). Ligand-bound and nuclear-localized AHR dimerizes with the aryl hydrocarbon nuclear translocator (ARNT) and this heterodimeric complex associates with specific DNA sequences termed dioxin response elements (DREs), altering expression of downstream genes such as cytochrome P4501A1 (CYP1A1; Sutter and Greenlee, 1992; Sutter *et al.*, 1991). Both AHR expression and ligand activation of the AHR appear to be essential for the manifestation of much of TCDD developmental toxicity in mammals, since AHR null mice exhibit few signs of TCDD toxicity (Fernandez-Salguero *et al.*, 1996; Mimura *et al.*, 1997; Peters *et al.*, 1999). The zebrafish AHR signal transduction pathway is generally similar to that of mammals

¹ To whom correspondence should be addressed at School of Pharmacy, University of Wisconsin, 777 Highland Ave., Madison, WI 53705–2222. Fax: (608) 265-3316. E-mail: repeterson@pharmacy.wisc.edu.

with the notable exception that fish possess at least two AHR genes while mammals have only one (Hahn *et al.*, 1997).

Two distinct classes of AHR genes (*AHR1* and 2) have been identified in fish (Hahn *et al.*, 1997). Phylogenetic comparisons suggest that the 2 forms of fish AHR arose from a gene duplication event during fish evolution (Hahn *et al.*, 1997). Sequence analysis reveals that *zfAHR1* shares the greatest sequence similarity with the mammalian AHRs (Andreasen *et al.*, 2002). The nomenclature of the fish AHRs and ARNTs used here follows the evolutionary conventions suggested in recent reports (Hahn *et al.*, 1997). An ARNT1 has not been identified in fish, however, *rtARNTb* identified in rainbow trout shares sequence homology with both ARNT and ARNT2 (Pollenz *et al.*, 1996; Powell and Hahn, 2000). Full-length zebrafish AHR2 (*zfAHR2*) and ARNT2 (*zfARNT2*) cDNAs have been cloned and their translation products characterized (Tanguay *et al.*, 1999, 2000). Four splice variants of *zfARNT2* (*zfARNT2a*, *zfARNT2b*, *zfARNT2c*, and *zfARNT2x*) have been identified. Only *zfARNT2b* has been demonstrated to be transcriptionally active with *zfAHR2*. *zfAHR2* and *zfARNT2b* form a functional heterodimer *in vitro*. The *zfAHR2/zfARNT2b* complex specifically recognizes DREs in gel shift experiments and induces DRE driven transcription in response to TCDD exposure in COS-7 cells (Tanguay *et al.*, 1999, 2000). A full-length *zfAHR1* corresponding to a partial fragment previously described by Wang and coworkers (Wang *et al.*, 1998) also has been cloned and characterized (Andreasen *et al.*, 2002).

The similar signs of developmental TCDD toxicity observed across fish species suggest there is a common mechanism of toxicity among fish (Walker and Peterson, 1994). In larval fish this mechanism is hypothesized to involve AHR, since the earliest signs of TCDD toxicity correlate with expression and activation of AHR in trout and zebrafish larvae (Guiney *et al.*, 1997; Henry *et al.*, 1997; Tanguay *et al.*, 1999). Furthermore, the ability of various PCDD, PCDF, and PCB congeners to activate the AHR pathway is correlated with their potency as mediators of TCDD-like developmental toxicity in rainbow trout (Walker and Peterson, 1991; Zabel *et al.*, 1995, 1996). If the AHR is required for TCDD toxicity, components of the AHR signaling pathway in zebrafish larvae should be expressed and active in tissues directly responsive to TCDD. Identifying these tissues and the onset of AHR activity could provide insight into the initiating events of TCDD developmental toxicity. In previous work we qualitatively determined the expression of *zfAHR2*, *zfARNT2b*, and *zfCYP1A* mRNAs isolated from extracts of zebrafish larvae (Tanguay *et al.*, 1999, 2000).

Objectives of the present study were to: (1) quantify the expression of *zfAHR2*, *zfARNT2a*, *zfARNT2b/c*, and *zfCYP1A* mRNAs during larval development in zebrafish, (2) assess the effect of TCDD exposure on abundance of these mRNAs, (3) determine if the transcripts are colocalized particularly in larval tissues involved in TCDD toxicity, (4) determine if TCDD exposure alters the temporal and/or spatial

expression of the mRNAs, and (5) identify larval tissue where AHR activation by TCDD has occurred based on positive immunofluorescence for *zfCYP1A*. Unfortunately tissue specific expression pattern of *zfAHR1* in embryos and larvae could not be determined due to low tissue abundance. To address these objectives vehicle (control) and TCDD exposed zebrafish embryos and larvae were assessed at designated times of development from 12 to 120 h postfertilization (hpf). Since the cardiovascular system is a target of TCDD toxicity in zebrafish larvae, expression of the AHR regulated gene *zfCYP1A*, and *zfAHR2*, *zfARNT2a*, and *zfARNT2b/c* were investigated beginning at 12 hpf. This is prior to initiation of the heartbeat at 24 hpf and before the first signs of TCDD developmental toxicity are manifested at 72 hpf. Previous studies using high exposure concentrations of TCDD found that *zfCYP1A* mRNA was induced as early as 24 hpf (Tanguay *et al.*, 1999), but the specific tissues in which the expression occurred was not known. Also it was uncertain if the AHR pathway would be activated by TCDD in zebrafish larval tissues in which toxicity was manifested, and if increased *zfCYP1A* expression in these tissues would precede the earliest occurring signs of toxicity, namely pericardial edema, reduced trunk blood flow, impaired lower jaw development, and reduced growth at 72 hpf (Henry *et al.*, 1997; Teraoka *et al.*, 2002). In the present study we demonstrate that expression of mRNAs for *zfAHR2*, *zfARNT2a*, *zfARNT2b/c*, and *zfCYP1A* occur during embryonic and larval development, that *zfCYP1A* protein is highly expressed in the cardiovascular system of larvae following TCDD exposure, that *zfAHR2* and *zfARNT2* mRNAs have similar, but not completely overlapping expression patterns, and that transcripts of *zfAHR2* and *zfARNT2* are found in larval tissues that are involved in TCDD toxicity and that respond to TCDD by induction of *zfCYP1A*.

MATERIALS AND METHODS

Static exposure of zebrafish embryos to waterborne TCDD. For *in situ* hybridization 1000 zebrafish embryos (AB strain, Eugene, OR) at 3 hpf with intact chorions were statically exposed for 1 h to either acetone vehicle (control) or an LC₁₀₀ concentration of TCDD (1.55 nM or 0.5 µg/l) dissolved in acetone (0.1 % v/v). This concentration of TCDD was chosen to ensure that the AHR signaling pathway would be activated in all responsive tissues to such an extent that *zfCYP1A* mRNA could be detected by *in situ* hybridization. Following the 1 h TCDD exposure all embryos were washed 3 times with TCDD-free water. Vehicle- and TCDD-exposed embryos were randomly culled to 100 for isolation at different time points and reared in 150-mm culture plates containing TCDD-free water at 28°C. Culture media was changed twice daily. One hundred control and TCDD-exposed larvae were euthanized with tricaine methanesulfonate (MS-222, 40 mg/l) and fixed overnight at 4°C in 4% paraformaldehyde in PBS at 12, 18, 24, 36, 48, 72, 96, and 120 hpf. This time course allowed TCDD-exposed larvae to exhibit signs of toxicity without losing significant numbers to mortality, which began around 144 hpf. Fixed larvae were dehydrated in a graded series of methanol solutions and stored in 100% methanol at -20°C. Fifty control and TCDD-exposed larvae were raised for 14 days to confirm that 100% mortality was caused by TCDD. Embryos were exposed to TCDD in this manner on at least 3 separate occasions for *in situ* mRNA analysis. For quantification of mRNA abundance embryos were

exposed to vehicle or TCDD as described above; however, more replicates with fewer individuals were exposed. For this experiment 5 groups of vehicle (control) and 5 groups of TCDD-exposed zebrafish larvae (50 larvae/group) were euthanized at each of the following times: 24, 36, 48, 72, and 120 hpf, frozen in liquid nitrogen, and stored at -70°C for RNA isolation and real-time PCR quantification of mRNAs. Additionally whole RNA was isolated from adult zebrafish as a reference for relative mRNA abundance. Embryos and larvae used for whole mount immunohistochemical analysis were exposed to vehicle control or TCDD as above with 6 individuals per time point (24, 36, 48, 72, and 120 hpf) and treatment.

Time course of *zfAHR2*, *zfARNT2a*, *zfARNT2b/c*, and *zfCYP1A* mRNA abundance. Total RNA was isolated from vehicle control and TCDD treated groups of fish ($n = 50/\text{group}$). Tissues were shredded using glass beads according to the manufacturer and RNA was isolated using a Qiasphere homogenizer (Qiagen, Chatsworth, CA). One μg of total RNA from each group was resolved on a 1% denaturing formaldehyde agarose gel to ensure quality and concentration of the RNA. cDNA was prepared from 2 μg of RNA per group using Superscript II (Life Technologies, Gaithersburg, MD) and oligo dT primers in a 20 μl volume. Quantitative PCR using gene specific primers was conducted using the Light CyclerTM (Roche, Indianapolis, IN). Specifically, 1 μl of each cDNA pool was used for each PCR reaction in the presence of SYBR Green, according to the manufacturer's instructions. Agarose gel electrophoresis and thermal denaturation (melt curve analysis) were used to confirm specific product formation.

Oligonucleotides. All oligonucleotide primers were synthesized by the University of Wisconsin Biotechnology Center and are written 5' to 3', F indicates forward primers corresponding to sense strands while antisense reverse primers are designated with an R. Primers for *zfAHR2* and *zfARNT2* subcloning were: *zfAHR2F1*, gcttcgcaaccagaattc; *zfAHR2R1*, cctagaagttgagtttaaacg; *zfARNT2F*, catttacagaaccgagcaaaa; *zfARNT2R*, cacagtgaatattccttgatc. Oligonucleotides for real-time PCR were: β -actinF, aagcaggagtagcatgagtc; β -actinR, tggagctcctcatgcatg; *zfAHR2F2*, acggtgaagctctcccata; *zfAHR2R2*, agtaggttctctgcccac; *zfARNT2F2*, gactgaattccttgcgcccac; *zfARNT2b/cR*, ctggagctgctgacgttg; *zfARNT2aR*, cacagtgaatattccttgatc; *zfCYP1A*, tgccgattcatccctttcc; *zfCYP1R*, agagccgtgctgatagtg.

Probes for *in situ* hybridization. A fragment of the 3' end of *zfAHR2* was amplified using primers *zfAHR2F1* and *zfAHR2R1* and subcloned into pGEM-T EASY vector (Promega, Madison, WI). A fragment containing the 5' end of *zfARNT2* was generated using primers *zfARNT2F* and *zfARNT2R* and subcloned into pGEM-T EASY vector. A partial *zfCYP1A* clone was obtained from Dr. C. H. Hu of National Taiwan Ocean University. The *zfCYP1A* sequence shared 79% amino acid identity with the rainbow trout CYP1A (gene bank accession number U62796). *zfAHR2*, *zfARNT2*, and *zfCYP1A* specific digoxigenin-UTP riboprobes were generated from linearized vectors. The *zfAHR2* riboprobes corresponded to position bp +2236 to 4147 within the C-terminus of the cDNA (Fig. 1). The *zfARNT2* riboprobes (bp -108 to +813) encompass part of the 5' UTR and most of the PAS B domain (Fig. 1). The 1107 bp *zfCYP1A* digoxigenin-UTP riboprobe (bp +159 to 1266) corresponds to the rainbow trout amino acids 53 to 422 of the 522 amino acid full-length protein (Fig. 1).

Whole mount *in situ* hybridization of *zfAHR2*, *zfARNT2a/b/c*, and *zfCYP1A*. Whole mount *in situ* hybridization was conducted with both sense and antisense digoxigenin RNA probes that were visualized with anti-digoxigenin Fab fragments conjugated with alkaline phosphatase (Roche Molecular Biochemicals) according to standard methods (Westerfield, 1995). All hybridization was conducted at 62°C . The riboprobe hybridization concentration of *zfAHR2* and *zfARNT2a/b/c* was 1.25 $\mu\text{g}/\text{ml}$ and *zfCYP1A* was hybridized at 500 ng/ml. At least 15 individual organisms were examined for each riboprobe within a treatment group. Images are representative of at least 3 separate TCDD or vehicle exposure experiments. Localization of mRNA expression was confirmed by sectioning embryos and larvae after whole mount *in situ* hybridization. Embryos and larvae were embedded in paraffin and sectioned. Five μm sections were then deparaffinized and counter-stained with nuclear fast red. The scoring system used to evaluate staining intensity was: 0 = not

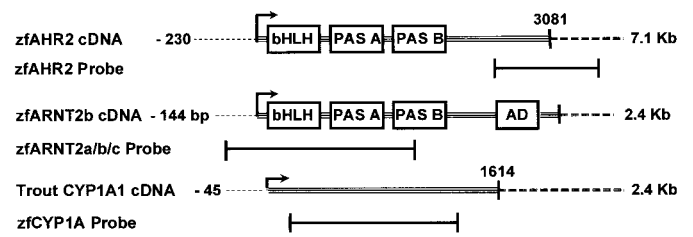


FIG. 1. Alignment of riboprobe sequences with known translated gene sequences. AHR and ARNT domains; basic helix loop helix (bHLH); PAS; AD, transactivation domain. Length of riboprobes; *zfAHR2* 1911 base pairs, *zfARNT2* 921 base pairs, *zfCYP1A* 1107 base pairs. Dashed line, 5' UTR; triple solid line, translated sequence; double dashed line, 3' UTR; single solid line, riboprobe sequence; arrow, translation start site.

detected, 1 = light stain, 2 = moderate stain, and 3 = intense stain. Other larvae were frozen, sectioned, and stained prior to light microscopic analysis and evaluation of staining intensity.

Whole mount immunolocalization of *zfCYP1A*. The tissue distribution of *zfCYP1A* protein in zebrafish embryos and larvae was determined using the monoclonal antibody MAb 1-12-3 (Park *et al.*, 1986). Stegeman and coworkers have used this antibody to specifically detect CYP1A in several fish species (Guiney *et al.*, 1997; Iwata and Stegeman, 2000; Schlezinger and Stegeman, 2000; Smolowitz *et al.*, 1992; Stegeman *et al.*, 1989, 2001; Van Veld *et al.*, 1997). TCDD-exposed and vehicle control embryos were fixed overnight in 4% paraformaldehyde in PBS and washed in PBS + 0.1% Tween-20 (PBST). Larvae were permeabilized with -20°C acetone for 20 min and rinsed in PBST before digestion with collagenase (1 mg/ml) for 30–90 min. Permeabilized larvae were blocked in 10% normal calf serum in PBST before addition of MAb 1-12-3 (0.3 $\mu\text{g}/\text{ml}$). Following several 10 min washes with PBST, larvae were incubated with a secondary antibody, (Alexa-488 conjugated goat anti-mouse, Molecular Probes, Eugene, OR) for 5 h at 22°C . Tissues were then washed 3 times for 10 min in PBST and visualized by epifluorescence microscopy.

Imaging. Whole mount *in situ* images were visualized using a Wild M8 stereomicroscope or a Nikon OPTIPHOT-2 compound microscope attached to a Sony CCD color camera. Video images were captured using Image Pro Plus software (Media Cybernetics, Silver Springs, MD). Fluorescent immunohistochemistry images were digitally captured using a MicroMax 5 Mhz camera (Princeton Instruments, Trenton, NJ).

Statistical analyses. Gene-specific mRNA abundance was determined at designated times of development from 5 groups of zebrafish larvae (50 larvae/group) exposed to either vehicle or TCDD, respectively. Abundance of mRNAs detected by quantitative real-time PCR was expressed as mean \pm SE. Significance of stage of development and TCDD exposure on *zfAHR2*, *zfARNT2a*, *zfARNT2b/c*, and *zfCYP1A* mRNA abundance was assessed by two-way analysis of variance on \log_{10} transformed data. Differences between groups were analyzed by the Tukey method with significance set at $p < 0.05$.

RESULTS

Time Course of *zfCYP1A*, *zfAHR2*, *zfARNT2a*, and *zfARNT2b/c* mRNA Expression in Whole Body Extracts of Larvae Exposed to Vehicle or TCDD

RNA was isolated from vehicle-exposed zebrafish at different stages of embryonic and larval development and the abundances of *zfCYP1A*, *zfAHR2*, *zfARNT2a*, and *zfARNT2b/c* mRNAs were determined relative to β -actin mRNA abundance

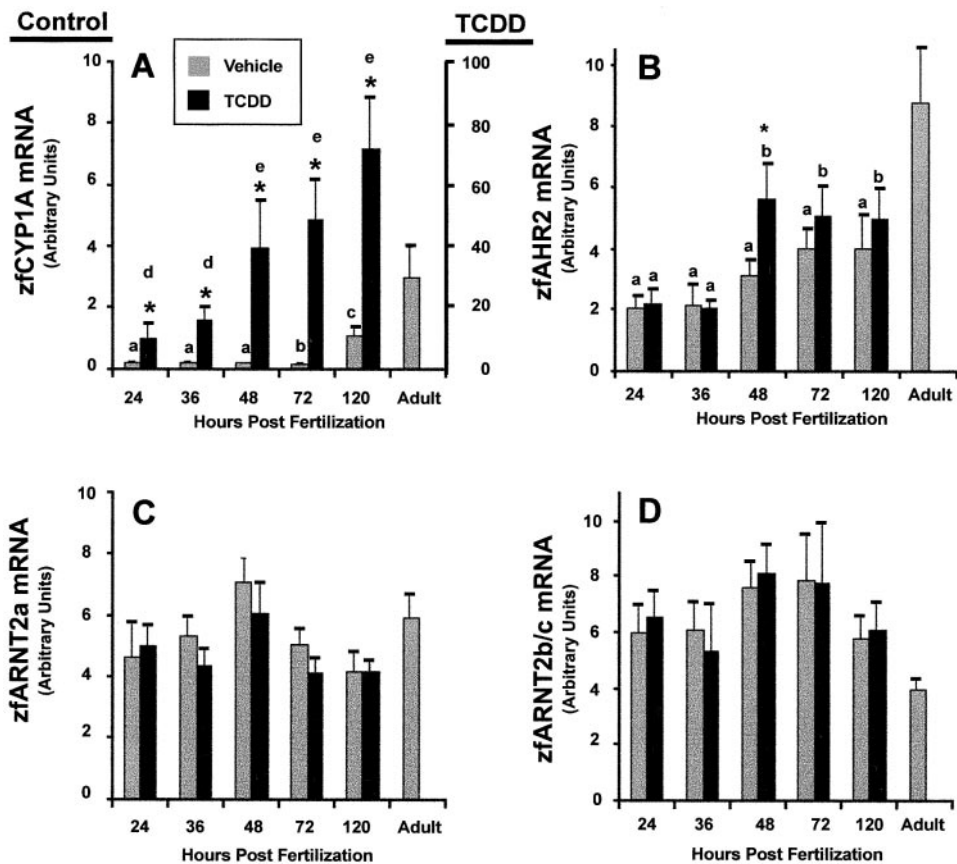


FIG. 2. Time course of zfAHR2, zfARNT2a, zfARNT2b/c, and zfcYP1A mRNA expression in vehicle- and TCDD-exposed zebrafish larvae by quantitative real-time PCR. Gene specific primers were used to quantify mRNAs for: zfcYP1A (A), note that the scale of the ordinate for the vehicle-treated larvae (left) is 1/10th of that for the TCDD-treated larvae (right); zfAHR2 (B), zfARNT2a (C), and zfARNT2b/c (D). Samples were run concurrently with standard curves derived from plasmid cDNA dilutions for each primer set. Values for each primer pair were normalized to β -actin mRNA levels. Each bar represents mean \pm SE, $n = 5$. *Significantly different from vehicle (control) at the same time ($p < 0.05$).

(Fig. 2, shaded bars, panels A, B, C, and D). In addition, the effect of exposing zebrafish embryos (3–4 hpf) to an LC₁₀₀ concentration of TCDD on expression of these same messages was assessed (Fig. 2, solid bars, panels A, B, C, and D). The abundance of each mRNA was also assessed in whole adult extracts as a reference for relative abundance in the whole adult. Additionally the detection of each mRNA in the adult served as a positive control for the assay. Quantitative real-time PCR was used to measure mRNA abundance. More specifically, standard curves allowed assignment of relative concentrations to zfcYP1A, zfAHR2, zfARNT2a, and zfARNT2b/c mRNAs and these values were normalized to zebrafish β -actin mRNA abundance at each developmental time as a control for mRNA recovery and reverse transcription efficiency. While differences in primer hybridization efficiency prevent the measurement of one mRNA species from being compared to another, general trends in relative mRNA abundance are observable. For the genes evaluated in Figure 2 relative mRNA abundance (from highest abundance to lowest abundance) followed the general trend: zfcYP1A (TCDD) > zfAHR2 (TCDD, vehicle), zfARNT2b/c (TCDD, vehicle), zfcYP1A (vehicle) \gg zfARNT2a (TCDD, vehicle). Essentially the same trend was observed for the relative abundance of these messages in Northern blot analyses of zebrafish larvae extracts (Tanguay *et al.*, 1999, 2000).

In vehicle-exposed zebrafish embryos, low constitutive expression of zfcYP1A mRNA was detected at 24 hpf with elevated expression at 120 hpf (Fig. 2A). Note in Figure 2A that the left ordinate is for the vehicle-exposed group and that its scale is 1/10th of that for TCDD-exposed group shown on the right ordinate. TCDD exposure caused elevated expression of zfcYP1A, relative to that in the vehicle (control) group, from 24 to 120 hpf (Fig. 2A). zfAHR2 mRNA was also detected in vehicle-exposed zebrafish embryos and larvae from 24 to 120 hpf (Fig. 2B). zfAHR2 relative mRNA abundance in the TCDD treatment group was similar to the control group at 24, 36, 72, and 120 hpf. However, at 48 hpf TCDD exposure caused a significant increase in zfAHR2 message. To quantify the levels of zfARNT2 splice variants, 2 sets of primers were used. One set amplified only zfARNT2a and another amplified both zfARNT2b and zfARNT2c. The mRNA splice variants of zfARNT2, namely zfARNT2a and zfARNT2b/c, were detected at 24 hpf with very little change in expression through 120 hpf (Figs. 2C and 2D). zfARNT2a (Fig. 2C) was expressed at much lower levels than zfARNT2b/c. This indicates that the contribution of zfARNT2a to the *in situ* localization of zfARNT2 mRNAs (shown later in Fig. 11) was minimal. Finally, the relative abundance of zfARNT2a and zfARNT2b/c mRNA splice variants were not altered significantly by embryonic exposure to TCDD (Figs. 2C and 2D).

Tissue-Specific Expression of zfCYP1A Protein and mRNA in Larvae Exposed to Vehicle or TCDD

The developmental and tissue specific expression of zfCYP1A mRNA and protein in vehicle- and TCDD-exposed embryos and larvae at 24, 36, 48, and 120 hpf is summarized in Table 1. zfCYP1A protein was detected in whole mount embryos and larvae immunohistochemically and is denoted by gray shaded cells. zfCYP1A mRNA was detected by whole mount hybridization with an antisense zfCYP1A mRNA probe. Localization of zfCYP1A mRNA was verified histologically in sectioned embryos and larvae that were hybridized with the antisense zfCYP1A mRNA. The intensity of riboprobe signal detected in sectioned tissues was scored with 0 being no detection; 1, light; 2, moderate; and 3, very intense expression. When the intensity of zfCYP1A mRNA expression was different between organisms in the same treatment and age group the average intensity was reported. For each riboprobe, the difference between individual organisms never varied by one unit on this scale. In some cases zfCYP1A mRNA was detected in whole mount embryos and larvae but not upon sectioning due to low expression and or size of the tissue. An asterisk indicates positive zfCYP1A mRNA expression when this occurred.

In vehicle (control) zebrafish embryos and larvae, constitutive expression of zfCYP1A mRNA and protein was essentially undetected until 120 hpf where it is primarily localized in tissues of meso- and endodermal origin at low levels (Table 1). In tissues derived from ectoderm there was no expression of zfCYP1A protein detected at any time from 24 to 120 hpf. Message for zfCYP1A was only detected at very low levels in the ear and vent. In tissues derived from mesoderm in the vehicle (control) group, zfCYP1A mRNA and protein were detected at low levels in the vasculature of the head, trunk, and tail and message was detected at a low level in the heart. In tissues derived from endoderm in vehicle-exposed zebrafish, expression of zfCYP1A mRNA and protein was detected in the intestinal tract at 120 hpf and message was expressed at a low level in the oropharyngeal mucosa and vent.

TCDD exposure markedly increased the diversity of tissues expressing zfCYP1A mRNA and protein with the ectoderm-, mesoderm-, and endoderm-derived tissues all expressing zfCYP1A in all zebrafish embryos and larvae examined (Table 1). TCDD exposure also resulted in earlier developmental expression of zfCYP1A message and protein. In tissues derived from ectoderm, zfCYP1A message and protein was induced in the skin of the head, trunk, and tail. Additionally TCDD strongly induced zfCYP1A mRNA in the neuroepithelium of the ear at 48 and 120 hpf, however, protein could not be positively detected in whole mount tissues since larvae were not sectioned after whole mount immunohistochemical analysis. In the mesoderm, zfCYP1A mRNA preceded protein detection in the vasculature being expressed as early as 24 hpf in head, trunk, and yolk sac blood vessels. Expression of zfCYP1A mRNA was also observed following TCDD expo-

sure in the head and trunk kidney at 36, 48, and 120 hpf. The zfCYP1A protein could not be readily detected in the kidney since the tissues were not sectioned, but kidney expression was detected by *in situ* hybridization. Endodermal expression of zfCYP1A protein and mRNA was detected in the intestinal mucosa and anal vent of the enteric tract at 48 and 120 hpf. Lastly, the liver of TCDD-exposed larvae expressed high levels of zfCYP1A protein and mRNA at 48 and 120 hpf.

Whole Mount Immunolocalization of zfCYP1A in Larvae Exposed to TCDD

The specificity of immunolocalization was ensured by the lack of signal in embryos incubated without the CYP1A antibody (Mab 12-3-1) but with the secondary antibody, Alexa-488 (data not shown). Specific immunolocalization of zfCYP1A was difficult to detect prior to 72 hpf due to autofluorescence of the yolk. zfCYP1A protein was first detected in TCDD-exposed larvae at 36 hpf (Fig. 3A) as fluorescence in the anal and urinary pores (AP, UP; Fig. 3B), developing vasculature of the tail including the caudal artery and vein (CA, CV), and intersegmental vessels (SE; Fig. 3B), and as a punctate pattern of fluorescence in the skin (Fig. 3C). In TCDD-exposed zebrafish larvae at 48 hpf (Fig. 3D) and 72 hpf (Fig. 3F), zfCYP1A immunofluorescence was evident in the vasculature throughout the embryo including the intersegmental vessels (SE), caudal artery and vein (CA, CV), dorsal aorta, pectoral vasculature, gill arches and vessels in the head (BA) as well as in the anal and urinary pores (AP, UP; Figs. 3D, 3E, and 3F). Since the heart overlays the yolk sac, specific zfCYP1A localization of the heart could not be determined until the heart separated from the yolk sac at 72 hpf.

Constitutive expression of zfCYP1A protein was detected in vehicle-exposed zebrafish larvae at 120 hpf in all individuals examined (Fig. 4A). In this representative larva weak zfCYP1A immunofluorescence was observed in the head, gastrointestinal tract, and vasculature throughout the body. These findings were consistent with the time course of zfCYP1A mRNA expression measured by real-time PCR and by whole mount *in situ* hybridization results both of which demonstrated that zfCYP1A message was only weakly expressed in vehicle-exposed larvae at 120 hpf and was localized in the gastrointestinal tract (Fig. 2A, Figs. 8E–F, Table 1). In sharp contrast, embryonic exposure to TCDD resulted in elevated levels of zfCYP1A protein in zebrafish larva at 120 hpf (Figs. 4B–D). The most predominate tissue in which increased zfCYP1A expression occurred was the vascular endothelium throughout the body (Figs. 4B–D). The lateral view of this TCDD-exposed larva shows vascular specific detection of zfCYP1A in the head, trunk, and tail (Fig. 4B). The lateral and ventral views demonstrate that zfCYP1A was also immunolocalized to the heart, liver, and enteric tract of the TCDD treated larva (Figs. 4B–C).

Evaluation of the immunofluorescence for zfCYP1A in individual blood vessels in various regions of the head of a representative TCDD-exposed zebrafish larva at 120 hpf is

TABLE 1
Tissue Specific Expression of zfCYP1A mRNA and Protein from 24 to 120 h Postfertilization (hpf)
in Vehicle Control and TCDD-Exposed Zebrafish Larvae

	Region	Organ System	Organ	Tissue	Control (hpf)				TCDD (hpf)				
					24	36	48	120	24	36	48	120	
Ectoderm	Head	Skin		Malpighian Cell					*	*	1*		
			Sensory Organ	Ear ^a	Internal Neuro-epithelial Layer			1				2.5	2
	Trunk	Skin	Dorsal Aspect	Malpighian Cell					1*	1*	1*		
			Vent	Malpighian Cell			1		*	*	*	2*	
		Pectoral Fin	Skin	Malpighian Cell							*	1*	
	Tail	Skin	Dorsal Aspect	Malpighian Cell					1*	1*	1*		
	Yolk Sac	Skin	Entire Yolk Sac	Malpighian Cell					*	*	*		
			Caudo-dorsal	Malpighian Cell					1*	1*	1*		
			Hatching Glands ^b							1*	*		
	Mesoderm	Head	Vascular	Vessels	Endothelium		1		1	2	2.5*	2.5*	2.5*
Meninges ^b												2	
				Head Kidney ^a	Mesenchyme						2	2	2
Trunk		Vascular	Heart	Endocardium									2.5
				Pericardium				1					2.5
			Vessels	Endothelium		1			2*	2.5*	2.5*	2.5*	
		Entire Trunk		Peritoneum				1				2	
		Urinary Tract	Trunk Kidney	Mesenchyme						2	2	2	
		Hematopoietic									2		
		Renal Tubules										2	
Tail	Vascular	Vessels	Endothelium						2*	2.5*	2.5*		
Yolk Sac	Vascular	Vessels	Vitelline					2	2.5*	2.5*	2.5*		
Endoderm	Head	Pharynx		Oropharyngeal Mucosa			1	1			2	1	
	Trunk	Enteric Tract		Intestinal Mucosa				1			1	2.5*	
				Vent				1	*	*	1*	2*	
			Liver								2	3*	

Note. Numbers indicate intensity of *in situ* probe stain in sectioned tissues. Gray shaded cells indicate immunolocalization of zfCYP1A.

^amRNA and protein could not be detected without sectioning.

^bNeural crest contributes to both meninges and to dermal cartilage and bone of fins.

*mRNA detected in whole mount *in situ* hybridization.

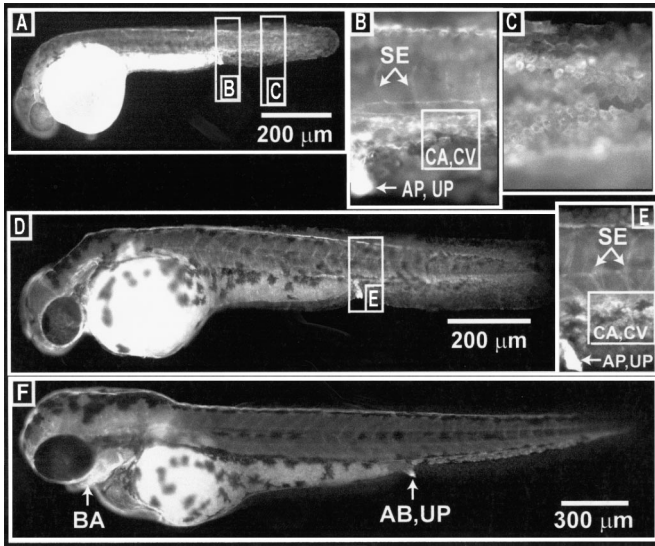


FIG. 3. Whole mount immunolocalization of zfCYP1A in TCDD-exposed larvae at 36 hpf (A, B, and C), 48 hpf (D and E), and 72 hpf (F) using MAb 1-12-3. The images are representative of 12 TCDD-exposed larvae from 2 exposure experiments. Original magnification $\times 200$ (B, C, and E). AP, anal pore; BA, branchial arches; CA, caudal artery; CV, caudal vein; SE, intersegmental vessel; UP, urinary pore.

shown in Figure 5. Vascular endothelium-specific zfCYP1A immunofluorescence was observed in essentially all vessels examined in the head including: branchial arches (BA), poste-

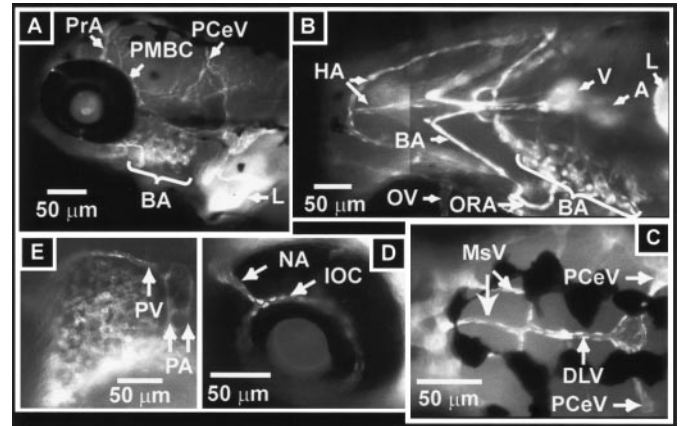


FIG. 5. Vasculature specific immunolocalization of zfCYP1A in a 120 hpf zebrafish larva exposed as a 3-h-old embryo to TCDD. (A) Lateral view of head; BA, branchial arches; L, liver; PCeV, posterior cerebral vein; PMBC, primordial midbrain channel; PrA, prosencephalic artery. (B) Composite view of 2 ventral images of the head; A, atrium; HA, hypobranchial artery; ORA, opercular artery; OV, optic vein; V, ventricle. (C) Dorsal view of the head; DLV, dorsal longitudinal vein; MsV, mesencephalic vein. (D) Lateral view of the eye; IOC, inner optic circle; NA, nasal artery. (E) Lateral view of the pectoral fin; PA, pectoral artery; PV, pectoral vein. The images are representative of 12 TCDD-exposed larvae from 2 exposure experiments.

rior cerebral vein (PCeV), primordial midbrain channel (PMBC), and prosencephalic artery (PrA; Fig. 5A, lateral view); branchial arches (BA), hypobranchial artery (HA), opercular artery (ORA), and optic vein (OV; Fig. 5B, ventral view); dorsal longitudinal vein (DLV), mesencephalic vein (MsV), and posterior cerebral vein (PCeV; Fig. 5C, dorsal view); inner optic circle (IOC) and nasal artery (NA) of the eye (Fig. 5D, lateral view); and pectoral artery (PA) and pectoral vein (PV) of the pectoral fin (Fig. 5E, lateral view).

Immunolocalization of zfCYP1A to the vascular endothelium in the trunk and tail regions of a representative TCDD-exposed zebrafish larva at 120 hpf is shown in Figure 6. In the trunk and tail, zfCYP1A was evident in the vascular endothelium of the dorsal aorta (DA), intersegmental vessels (SE), and posterior cardinal vein (Fig. 6A) and in the subintestinal vein (SIV; Fig. 6B). Figure 6 also reveals positive immunofluorescence for zfCYP1A in the kidney, intestine, and anal pore.

Immunofluorescent detection of zfCYP1A in the 120 hpf zebrafish larvae exposed to TCDD was also observed in the heart ventricle (V) and atrium (A; Fig. 7A) and in the liver (L) and hepatic portal vein (HPV; Fig. 7B).

Whole Mount in Situ Hybridization: Lack of Staining with Sense RNA Probes for zfCYP1A, zfAHR2, and zfARNT2a/b/c mRNAs

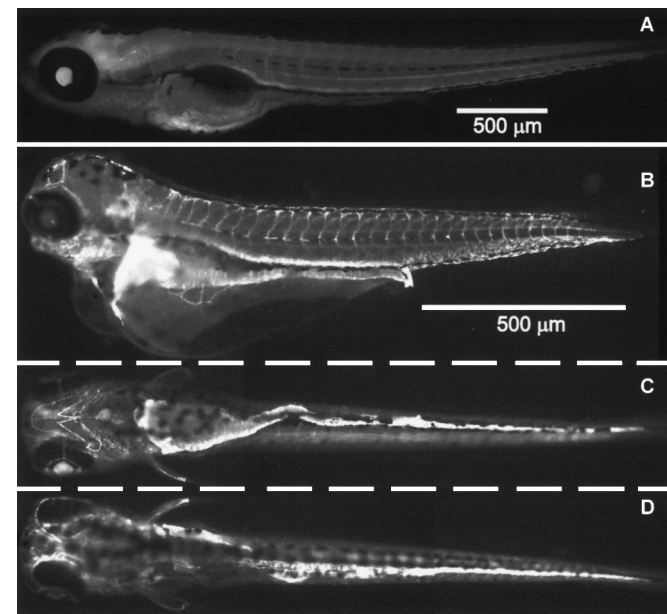


FIG. 4. Whole mount immunolocalization of zfCYP1A in a representative 120 hpf vehicle (control) larva and TCDD-exposed larva using MAb 1-12-3. Each larva was exposed to either vehicle (A, lateral view) or TCDD (B, lateral view; C, ventral view; and D, dorsal view) for 1 h as a 3-h-old embryo. In each panel 2 images of the same larva were digitally joined together to visualize the whole organism. The images are representative of 12 TCDD-exposed larvae from 2 exposure experiments.

Since high quality antibodies are not yet available to detect zfAHR2 and zfARNT2, whole mount *in situ* hybridization was used to assess the temporal and spatial expression of zfCYP1A, zfAHR2, and zfARNT2a/b/c mRNAs in zebrafish at 12, 18, 24,

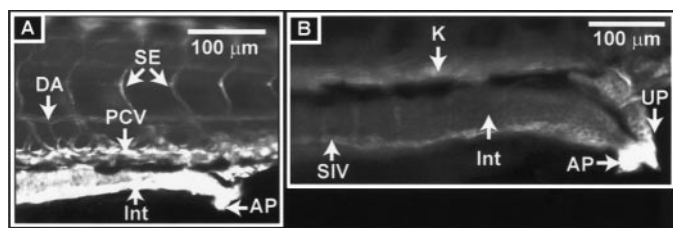


FIG. 6. Tissue-specific immunolocalization of zfCYP1A in the trunk of a 120 hpf zebrafish larva exposed to TCDD as a 3-h-old embryo. (A) Lateral view showing the tail (original magnification $\times 100$); AP, anal pore; DA, dorsal aorta; Int, intestine; PCV, posterior cardinal vein; SE, intersegmental vessel. (B) Lateral view of the posterior intestine and kidney (original magnification $\times 200$); AP, anal pore; K, kidney; Int, intestine; SIV, subintestinal vein; UP, urinary pore. The images are representative of 12 TCDD-exposed larvae from 2 exposure experiments.

36, 48, 72, 96, and 120 hpf. Antisense hybridization specificity was confirmed for each riboprobe using sense strand specific riboprobes and the tissue specificity and staining intensity for each probe was confirmed by sectioning the whole mount embryos and larvae. None of the control sense probes produced staining at any developmental stage or in any larval tissues except for the swimbladder. This lack of staining for sense strand AHR2 riboprobe is illustrated in zebrafish embryos and larvae at 12, 18, 24, 36, 48, and 96 hpf (Fig. 8).

zfCYP1A mRNA Localization in Larvae Exposed to Vehicle or TCDD

Constitutive zfCYP1A mRNA expression was not detected by whole mount *in situ* hybridization in vehicle-exposed zebrafish larvae until 96 hpf when it was observed by light blue staining in endoderm-derived tissues such as the liver and enteric tract (Fig. 9E, top). This finding is consistent with elevated constitutive expression of zfCYP1A mRNA being detected by RT-PCR in vehicle (control) larvae at 120 hpf. In contrast to the weak and limited expression of zfCYP1A mRNA expression in vehicle (control) larvae, expression was readily detected in zebrafish larvae exposed to TCDD (Fig. 9). Expression was first evident at 24 hpf in tissues of mesodermal and ectodermal origin including the dorsal aorta (DA), anal pore (AP), urinary pore (UP), and skin (Fig. 9A, bottom). By 36 hpf, zfCYP1A mRNA expression was elevated in blood vessels throughout the body including the caudal artery (CA), caudal vein (CV), common cardinal vein (CCV), dorsal aorta (DA), gill arches, head vasculature (HV), posterior cardinal vein (PCV), as well as in the hatching gland (HG; Fig. 9B, bottom). TCDD-induced zfCYP1A mRNA expression at 48 hpf was observed in tissues derived from ectoderm, mesoderm, and endoderm. Ectoderm derived tissues expressing zfCYP1A mRNA included the ear and skin associated with the head, trunk, tail, and yolk sac. Expression was also observed in mesoderm-derived tissues represented by the vasculature including the head vasculature (HV), fin vasculature including the pectoral vein (PV) and pectoral artery (PA), posterior

cardinal vein (PCV), caudal vein (CV), and caudal artery (CA). Endoderm derived tissues expressing zfCYP1A message included the mucosa associated with the anal pore (AP) and urinary pore (UP; Fig. 9C, bottom). The expression pattern at 48 hpf remained similar at 72 and 96 hpf and was dominated by vascular-specific localization. At 72 hpf this was represented by expression of zfCYP1A message in the branchial arches (BA), head vasculature (HV), and subintestinal veins (SIV; Fig. 9D, bottom) and at 96 hpf by expression in the branchial arches (BA; Fig. 9E, bottom). At 72 hpf expression of zfCYP1A mRNA was evident in the heart (H), anal pore (AP) and urinary pore (UP; Fig. 9D, bottom). By 96 hpf expression is much more evident in tissues of endodermal origin including the liver (L) and intestinal tract (Int) as well as in tissues of ectodermal origin such as the brain (BR) and ear (Fig. 9E, bottom). This pattern of zfCYP1A message expression persists at 120 hpf (Fig. 9F, bottom).

Tissue-Specific Expression of zfAHR2 and zfARNT2a/b/c mRNAs in Embryos and Larvae Exposed to Vehicle or TCDD

Tables 2 and 3 summarize the results for tissue-specific expression of zfAHR2 and zfARNT2a/b/c mRNAs from vehicle control and TCDD-exposed embryos and larvae that were hybridized with gene specific riboprobes at 24, 36, 48, and 120 hpf. Abundance and localization of mRNA expression was empirically determined histologically by sectioning embryos and larvae after whole mount *in situ* hybridization. The intensity of riboprobe signal detected in sectioned tissues was empirically noted with 0 being no detection; 1, light; 2, moderate; and 3, very intense expression. When the intensity of zfAHR2 or zfARNT2a/b/c mRNA expression was different between individual organisms in the same treatment and age group, the average intensity was reported. In some cases either zfAHR2 or zfARNT2a/b/c mRNA was detected in whole mount embryos and larvae but not detected histologically due to low expression and/or size of the tissue. An asterisk (*) in Tables 2 and 3 indicates positive zfAHR2 or zfARNT2a/b/c mRNA expression when this occurred. Shaded cells in Tables 2 and 3

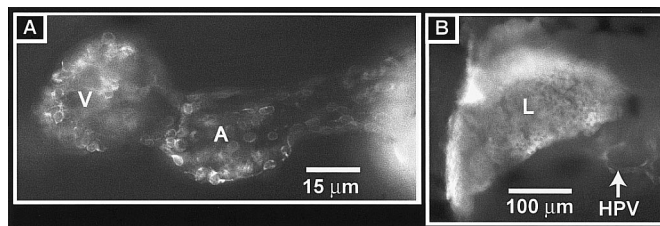


FIG. 7. Tissue-specific immunolocalization of zfCYP1A in a 120 hpf zebrafish larva exposed to TCDD as a 3-h-old embryo. (A) Ventral view showing specific localization in the heart; A, atrium and V, ventricle. (B) Lateral view showing immunolocalization in the liver (L) and hepatic portal vein (HPV). The images are representative of 12 TCDD-exposed larvae from 2 exposure experiments.

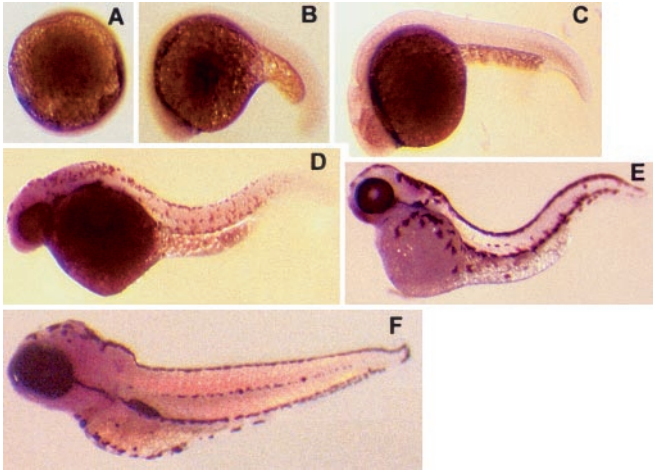


FIG. 8. Whole mount *in situ* hybridization using gene specific digoxigenin-labeled zfAHR2 sense RNA riboprobe ($n \geq 15$). Lateral views of larvae hybridized at (A) 12, (B) 18, (C) 24, (D) 36 (E) 48, and (F) 96 hpf.

indicate that TCDD-induced zfCYP1A protein and/or mRNA was detected in those particular tissues. Finally according to the *in situ* analysis there were essentially no differences in tissue-specific expression of either zfAHR2 or zfARNT2a/b/c mRNAs between vehicle and TCDD-exposed larvae at 24, 36, 48, or 120 hpf.² Therefore, scores for zfAHR2 and zfARNT2a/b/c mRNA expression intensity in the vehicle (control) and TCDD exposure groups were combined at 24, 36, 48, and 120 hpf (Tables 2 and 3).

zfAHR2 and zfARNT2a/b/c mRNAs were expressed in several tissues derived from ectoderm at 24, 36, 48, and 120 hpf (Table 2). In the head both transcription factors were expressed in the skin, brain, sensory organs including the eyes and ears and gill. Of the various positively staining structures in the head the highest expression of zfAHR2 and zfARNT2a/b/c messages were in the ears. In tissues derived from ectoderm in the trunk, tail, and yolk sac the expression of these 2 mRNAs was weak and occurred in the skin, spinal cord, and pectoral fins of the trunk, skin and caudal fin of the tail, and skin of the yolk sac. Expression of zfCYP1A protein or mRNA in response to TCDD exposure (shaded cells in Table 2) was more restricted than expression of zfAHR2 and zfARNT2a/b/c mRNAs. This was illustrated by colocalization of zfCYP1A, zfAHR2, and zfARNT2a/b/c occurring in only 2 ectoderm-derived tissues, the ears and skin.

Expression of mRNAs for zfAHR2 and zfARNT2a/b/c in tissues derived from mesoderm and endoderm was also observed in zebrafish larvae (Table 3). In general the expression of these messages in tissues of mesodermal and endodermal origin was weak and widespread. For zfAHR2 mRNA low expression was observed in mesoderm-derived tissues of the

² zfAHR2 mRNA was slightly induced by TCDD at 120 hpf in the pericardium and peritoneum of the trunk. Likewise zfARNT2a/b/c mRNA was induced by TCDD exposure at 120 hpf in the peritoneum.

head (blood vessels, meninges of the brain, and head kidney), trunk (heart, blood vessels, peritoneum, somites, lateral plate, and trunk kidney), tail (blood vessels, caudal fin, and somites), and yolk sac (blood vessels). For endoderm-derived tissues low expression of zfAHR2 mRNA was observed in the head (pharyngeal mucosa) and trunk (mucosa of the enteric tract and gall bladder) but was conspicuously absent from the liver. Expression of zfARNT2a/b/c generally followed the tissue distribution of zfAHR2 for mesoderm- and endoderm-derived tissues with certain exceptions. Most obvious was the greater expression of zfARNT2a/b/c in blood vessels, peritoneum, and caudal fin mesenchyme. Expression of zfCYP1A protein or mRNA in response to TCDD exposure (shaded cells in Table 3) was more restricted than expression of zfAHR2 and zfARNT2a/b/c mRNAs. Colocalization of zfCYP1A, zfAHR2, and zfARNT2a/b/c occurred in only 3 mesoderm-derived tissues, blood vessels,

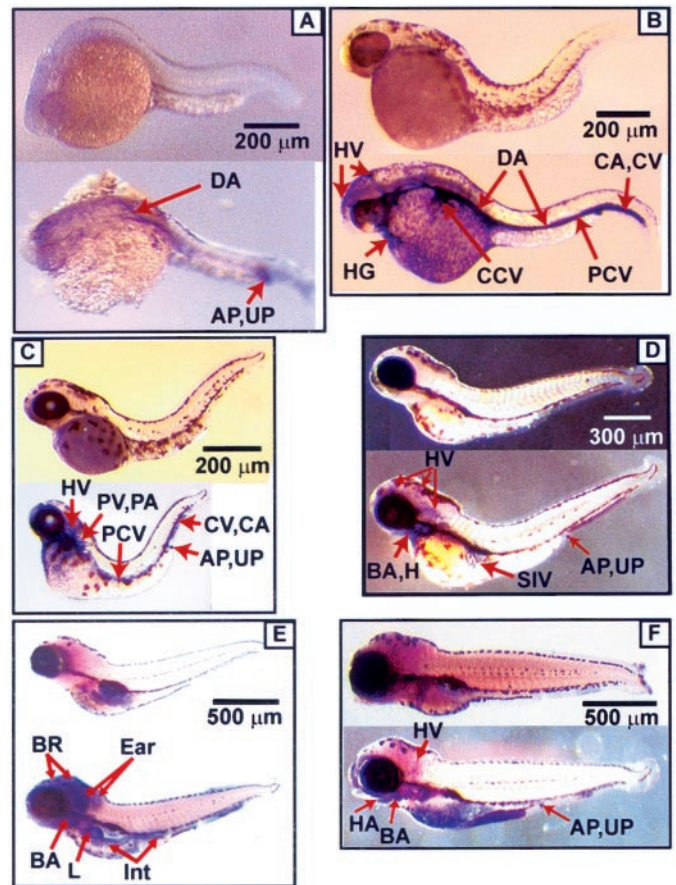


FIG. 9. Whole mount *in situ* hybridization using gene specific digoxigenin-labeled antisense RNA riboprobes for zfCYP1A ($n \geq 15$). Lateral views of larvae hybridized with the riboprobe at: (A) 24, (B) 36, (C) 48, (D) 72, (E) 96, and (F) 120 hpf. Embryos were exposed to vehicle (top) or TCDD (bottom) for 1 h at 3 hpf. AP, anal pore; BA, branchial arches; BR, brain; CA, caudal artery; CCV, common cardinal vein; CV, caudal vein; DA, dorsal aorta; H, heart; HA, hypobranchial artery; HG, hatching gland; HV, head vasculature; Int, intestine; L, liver; PA, pectoral artery; PCV, posterior cardinal vein; PV, pectoral vein; E, ear; SIV, subintestinal vein; UP, urinary pore.

TABLE 2
Tissue Specific Expression of zfAHR2, zfARNT2a/b/c mRNAs in Zebrafish from 24 to 120 h Postfertilization (hpf) and Colocalization with zfCYP1A mRNA and Protein

	Region	Organ System	Organ	Tissue	zfAHR2				zfARNT2			
					hpf				hpf			
					24	36	48	120	24	36	48	120
Ectoderm	Head	Skin		Malpighian Cell	1	1	1	1				1
			Brain	Neuroepithelium	1	1	1		1	1	1	
				Ependyma Lining Ventricles	1	1	1			1	1.5	
		Sensory Organs	Eye	Retinal Neuroepithelium	1	1	1		1	1	1	
				Lens Epithelium			1		1	1	1	1
			Ear	Internal Neuroepithelial	2	2	2	1	1	1	2.5	1
	Gill	Arch, Filaments, Lamellae	Surface Epithelium ^b				1				1	
	Trunk	Skin	Dorsal	Malpighian Cell	1	1	1	1				1
			Vent	Malpighian Cell		*	*					1.5
		Spinal Cord	Neuroepithelium	1	1	1		1	1	1		
		Pectoral Fin	Skin	Malpighian Cell		1	1.5	1			1	1
	Tail	Skin	Dorsal	Malpighian Cell	1	1	1	1				1
		Caudal Fin			1	1	1	1				1
	Yolk Sac	Skin	Entire Yolk Sac	Malpighian Cell	1				1	1		
			Caudo-dorsal	Malpighian Cell			1		1	1	1	
		Hatching Glands ^a	1.5				1.5					

Note. Numbers indicate intensity of *in situ* hybridization probe stain for zfAHR2 mRNA or zfARNT2a/b/c mRNA following sectioning of whole mount hybridized larvae. Gray shading indicates colocalization of zfCYP1A protein and/or mRNA.

^aMesoderm from dorsal axis near prechordal plate contributes to the hatching glands.

^bEndoderm may contribute to the surface epithelium of the gill.

*Indicates localization of zfAHR2 mRNA or zfARNT2a/b/c mRNA only in whole mount hybridized larvae.

heart, and trunk kidney. For endoderm-derived tissues only the enteric tract exhibited co-expression of zfCYP1A with zfAHR2 and zfARNT2a/b/c.

zfAHR2 mRNA Localization in Larvae Exposed to Vehicle or TCDD

Since there were essentially no differences between the vehicle (control) and TCDD treatment groups in zfAHR2

mRNA expression, whole mount *in situ* hybridization images of zebrafish embryos and larvae, representative of both groups, are shown at 12, 18, 24, 36, 48, 72, and 96 hpf, respectively (Fig. 10). At 12 hpf zfAHR2 was ubiquitously expressed in the embryo (Fig. 10A) but by 18 hpf increased expression of zfAHR2 mRNA was observed in the embryo trunk in the general region where hemangioblasts are found (Fig. 10B). By 24 hpf, zfAHR2 mRNA expression was observed in skin of the

TABLE 3
Tissue Specific Expression of zfAHR2, zfARNT2a/b/c mRNAs in Zebrafish from 24 to 120 h Postfertilization (hpf) and Colocalization with zfCYP1A mRNA and Protein

	Region	Organ System	Organ	Tissue	zfAHR2				zARNT2			
					hpf				hpf			
					24	36	48	120	24	36	48	120
Mesoderm	Head	Vascular	Vessels	Endothelium	1	*	1	1		1	1.5	1.5
		Entire Head		Mesenchyme	1	1	1		1	1	1.5	
		Meninges ^a				1						1
				Head Kidney	Mesenchyme		1	1				
	Trunk	Vascular	Heart	Endocardium			1.5				1	
				Myocardium			1.5					
				Pericardium			1.5	2		1	1	
			Vessels	Endothelium		*	*	*		1	1.5	1.5
		Entire Trunk		Peritoneum				2				3
				Mesenchyme					1	1	1.5	
		Somites				1	1	1		1		
		Lateral Plate				1	1	1		1	1	1
				Trunk Kidney	Mesenchyme		1	1				2
		Pectoral Fin			Mesenchyme			1				1
				Cartilage ^a			2				1	
				Skeletal Muscle							1	
	Tail	Vascular	Vessels	Endothelium		*	1			1	1.5	1.5
		Caudal Fin		Mesenchyme			1					3
		Somites		Mesenchyme			1		1			
	Yolk Sac	Vascular	Vessels	Vitelline			1			1	1.5	1.5
Entire Yolk Sac		Peri-vascular Tissue	Yolk Syncytial Cells	1				1				
Endoderm	Head	Pharynx		Oropharyngeal Mucosa			1	1		1	1	
	Trunk	Gut Anlage							1			
		Enteric Tract		Intestinal Mucosa				1		1		1
		Liver										1
		Gall Bladder						1				1
		Pancreas										1

Note. Numbers indicate intensity of *in situ* hybridization probe stain for zfAHR2 mRNA or zfARNT2a/b/c mRNA following sectioning of whole mount hybridized larvae. Gray shading indicates colocalization of zfCYP1A protein and/or mRNA.

^aNeural crest contributes to both meninges and to dermal cartilage and bone of fins.

*Indicates localization of zfAHR2 mRNA or zfARNT2a/b/c mRNA only in whole mount hybridized larvae.

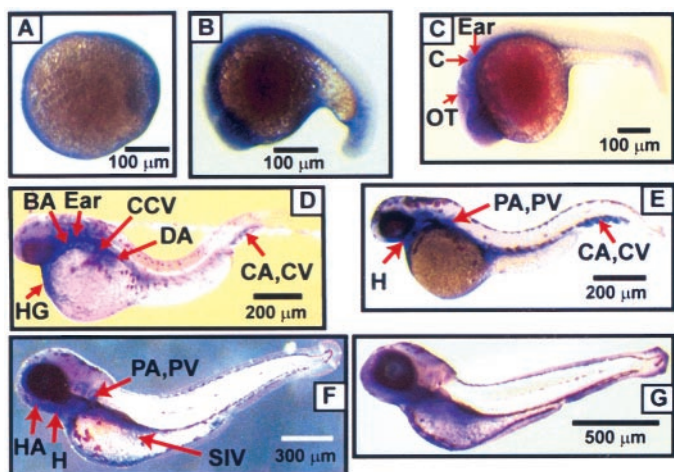


FIG. 10. Whole mount *in situ* hybridization using gene specific digoxigenin-labeled antisense RNA riboprobes for zfAHR2 ($n \geq 15$). Lateral views of larvae hybridized with the riboprobe at: (A) 12, (B) 18, (C) 24, (D) 36, (E) 48, (F) 72, and (G) 96 hpf. BA, branchial arches; C, cerebellum; CA, caudal artery; CCV, common cardinal vein; CV, caudal vein; DA, dorsal aorta; H, heart; HA, hypobranchial artery; HG, hatching gland; E, ear; OT, optic tectum; PA, pectoral artery; PV, pectoral vein; SIV, subintestinal vein.

head, trunk, tail, and yolk sac, regions of the brain including the optic tectum (OT) and cerebellum (C), spinal cord, and sensory organs including the eye and ear (Fig. 10C). Blood vessels throughout the larval body were found to express zfAHR2 at 36 hpf and they included the branchial arches (BA), caudal artery (CA), caudal vein (CV), common cardinal vein (CCV), and dorsal aorta (DA; Fig. 10D). The hatching gland (HG), ear, and anal pore also expressed zfAHR2 message at this time (Fig. 10D). At 48 hpf, zfAHR2 mRNA continued to be expressed in the vasculature and was detected in the heart (H) and in the pectoral artery (PA) and pectoral vein (PV) of the pectoral fin (Fig. 10E). At 72 hpf zfAHR2 was observed in the heart (H), hypobranchial artery (HA), subintestinal veins (SIV), and developing jaw (Fig. 10F). At 96 hpf the pattern of zfAHR2 mRNA expression was generally similar to that observed at 72 hpf (Fig. 10G). Expression of zfAHR2 message in the vasculature continued through 120 hpf, but expression in the brain, eyes, spinal cord, kidney, and trunk and tail somites (seen at earlier stages of development) was not detected at this time (Tables 2 and 3). However, zfAHR2 mRNA was detected in the intestinal mucosa and gall bladder at 120 hpf (Table 3).

zfARNT2a/b/c mRNA Localization in Larvae Exposed to Vehicle or TCDD

zfARNT2a/b/c mRNA expression was low at all stages of development and essentially unaffected by TCDD exposure. As with zfAHR2, zfARNT2a/b/c was expressed primarily in tissues of ectodermal and mesodermal origin. zfARNT2a/b/c mRNA expression was ubiquitously expressed in the zebrafish embryo at 12 hpf (Fig. 11A). At 18 hpf zfARNT2a/b/c expres-

sion was localized in the brain and spinal cord and was especially abundant in the forebrain including the olfactory rosette (Fig. 11B). At 24 hpf expression of zfARNT2a/b/c message was confined predominantly to the brain localizing in the olfactory placode (OP), telencephalon (T), optic tectum (OT), cerebellum (C), spinal cord (SC) and sensory organs including the eye and ear (Fig. 11C, lateral and dorsal views). At this time zfARNT2a/b/c mRNA was also observed in the hatching gland and yolk sac skin. By 36 hpf, expression continued in the central nervous system and could also be detected in the cardiovascular system including the pericardium of the heart and in blood vessels in the head, trunk, tail, and yolk sac (Fig. 11D). The expression pattern of zfARNT2a/b/c mRNA remained similar at 48 hpf with additional expression in the pectoral fin (Fig. 11E). Also the expression of zfARNT2a/b/c mRNA in the vasculature throughout the body of the zebrafish larva at 48 hpf was colocalized with zfAHR2 mRNA. At 72 hpf zfARNT2a/b/c message could be detected in the branchial arches (BA), developing jaw, and brain (Fig 11F). At 96 hpf zfARNT2a/b/c mRNA was expressed in vascular structures including the branchial arches (BA) and hypobranchial artery (HA) as well as the enteric tract including the intestine (Int; Fig. 11G).

DISCUSSION

Determining the expression pattern and abundance of zfAHR2 and zfARNT2 is crucial for understanding normal development in addition to determining a mechanistic understanding of TCDD developmental toxicity in zebrafish. Re-

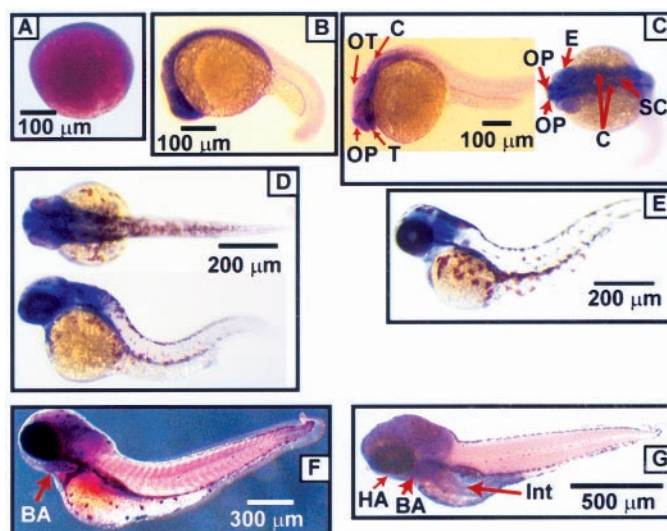


FIG. 11. Whole mount *in situ* hybridization using gene specific digoxigenin-labeled antisense RNA riboprobes for zfARNT2a/b/c ($n \geq 15$). Lateral or dorsal views of larvae hybridized with the riboprobe at: (A) 12, (B) 18, (C) 24, (D) 36, (E) 48, (F) 72, and (G) 96 hpf are shown. BA, branchial arches; C, cerebellum; HA, hypobranchial artery; Int, intestine; SC, spinal cord; OP, olfactory placode; OT, optic tectum; T, telencephalon.

search in laboratory mammals has demonstrated the necessity of AHR and ARNT2 for normal development. The AHR is required for normal vascular development in mice (Lahvis *et al.*, 2000; Schmidt *et al.*, 1996). In addition, developmental TCDD toxicity requires a functional AHR. Much of the developmental toxicity of TCDD is presumed to involve the AHR since developing mice lacking a functional AHR are insensitive to acute TCDD exposure (Fernandez-Salguero *et al.*, 1996; Mimura *et al.*, 1997; Peters *et al.*, 1999). ARNT2 is also important for normal development. Mice deficient in ARNT2 die within 24 h of birth and have impaired hypothalamic development (Hosoya *et al.*, 2001). In zebrafish ARNT2 may be necessary for normal development since over expression of a dominant negative, truncated splice variant of zfARNT2 (ARNT2 \times) alters development and is embryo lethal (Hsu *et al.*, 2001). The known members of the AHR pathway in zebrafish include zfAHR1, zfAHR2, and 4 zfARNT2 splice variants. For this study we chose to investigate the members that are functionally active in response to TCDD. zfAHR1 is not suspected to be involved in TCDD toxicity since it does not bind ligand efficiently, is not transcriptionally active with zfARNT2, and has a very limited tissue distribution (Andreasen *et al.*, 2002). Only 1 splice variant of zfARNT2, zfARNT2b, is known to be functionally active with zfAHR2 (Tanguay *et al.*, 2000). For these reasons it is implied that zfAHR2 and zfARNT2b are the functional members of the AHR pathway in zebrafish.

The findings from this study suggest that (1) zfAHR2, zfARNT2a, and zfARNT2b/c and zfCYP1A are all expressed early in development prior to the first signs of TCDD toxicity; (2) TCDD exposure has no effect on zfARNT2 abundance and only a marginal transient inductive effect on zfAHR2; (3) zfAHR2, zfARNT2 and TCDD induced zfCYP1A mRNAs colocalize in several tissues affected by TCDD exposure; (4) TCDD exposure has essentially no effect on the temporal and spatial localization of zfAHR2 and zfARNT2; and (5) immunolocalization of TCDD-induced zfCYP1A identified the cardiovascular and osmoregulatory systems as sites of active AHR signaling.

TCDD-Induced Cardiovascular Toxicity in Zebrafish Larvae

The cardiovascular system is a target of TCDD induced developmental toxicity in zebrafish (Henry *et al.*, 1997). In zebrafish larvae, exposed to TCDD at the embryonic stage of development, circulation is normal from onset of the beating heart at 24 hpf until about 72 hpf when it is first detected as being reduced in the trunk and tail (Henry *et al.*, 1997). Later in development a reduction in blood flow is observed in the head and gills (99 hpf), and is followed by reduced heart rate (125 hpf). TCDD-exposed larvae also show signs of pericardial edema, impaired lower jaw development, and reduced body growth by 72 hpf followed by yolk sac edema and reduced swimbladder inflation by 96 hpf. Mortality begins to occur at

144 hpf. Most of these signs of toxicity, with the notable exception of impaired lower jaw development (Teraoka *et al.*, 2002), are consistent with impaired cardiovascular function. Research in rainbow trout and lake trout larvae has shown that TCDD can impair heart development and increase vascular permeability leading to edema. This appears to involve activation of AHR signaling because the TCDD dose response relationship for increased CYP1A protein expression in the vascular endothelium of lake trout larvae was discovered to be similar to that for larval mortality (Guiney *et al.*, 1997). As with zebrafish, lake trout larvae exposed to TCDD exhibit circulatory failure and extensive edema prior to mortality. Furthermore, CYP1A expression in the vascular endothelium of lake trout larvae occurs prior to the onset of increased vascular permeability and edema (Guiney *et al.*, 2000). Expression of CYP1A in the vasculature of zebrafish larvae also occurs well before the onset of edema. A feature of the developmental cardio-toxicity in rainbow trout larvae is the finding that heart size is greatly reduced by TCDD (Hornung *et al.*, 1999). Thus, in zebrafish and trout larvae it is possible that either increased vascular permeability and/or reduced cardiac output could lead to reduced blood pressure and renal perfusion culminating in edema that is the hallmark sign of TCDD developmental toxicity in fish. A compromised cardiovascular system would result in reduced blood flow and may decrease the exchange of gases at the gills, swimbladder, and skin. Other signs of TCDD developmental toxicity in zebrafish and other fish could be accounted for by insufficient gas exchange promoting tissue necrosis, reduced growth, and inhibition of swimbladder inflation.

Abundance and Tissue Specific Expression of zfAHR2, zfARNT2, and zfCYP1A

Constitutive levels of zfCYP1A mRNA and protein were detected at 24 and 120 hpf respectively. This is earlier than the previously reported initial constitutive zfCYP1A mRNA and protein expression using northern and western analysis (Mattingly and Toscano, 2001; Tanguay *et al.*, 1999). The use of real time PCR and whole mount immunofluorescence allowed for detection of the previously unknown increase in the constitutive expression of zfCYP1A mRNA and protein at 120 hpf due to the sensitivity of the assays used. This correlates with the increase in constitutive aryl hydrocarbon hydroxylase or EROD activity observed after hatching in *Fundulus heteroclitus* and zebrafish respectively (Binder and Stegeman, 1984; Binder *et al.*, 1985; Mattingly and Toscano, 2001).

TCDD exposure induced the level of zfCYP1A expression in zebrafish embryos substantially at 24 hpf and it remained elevated thereafter. This indicates that TCDD activates the AHR pathway, potentially involving zfAHR2 and zfARNT2a/b/c, before the first signs of developmental toxicity are manifested. Whole mount immunolocalization of zfCYP1A protein was studied to identify potential sites of TCDD toxicity by

detecting tissues with an activated AHR pathway. Tissue and developmental stages expressing an active AHR signaling pathway were determined using a monoclonal antibody (Mab1-12-3) to detect zfCYP1A protein *in situ* at several developmental time points. TCDD induced zfCYP1A protein expression was first localized to the skin and developing vasculature of the zebrafish larva prior to the first signs of toxicity. The cardiovascular system, kidney, and liver of TCDD-exposed zebrafish larvae all expressed zfCYP1A protein by 120 hpf. This larval expression pattern is similar to that seen in *F. heteroclitus* (Toomey *et al.*, 2001). The tissue distribution of zfCYP1A in TCDD-exposed larvae at 120 hpf also resembles that seen in TCDD-exposed lake trout larvae and the adult pattern observed in several other fish species including zebrafish (Andreasen *et al.*, 2002; Buchmann *et al.*, 1993; Guiney *et al.*, 1997; Husoy *et al.*, 1994; Schlezinger and Stegeman, 2000; Smolowitz *et al.*, 1991, 1992; Stegeman *et al.*, 1989, 2001; Van Veld *et al.*, 1997). The use of zfCYP1A mRNA and protein localization as biomarkers of a TCDD activated AHR pathway has demonstrated, like in the lake trout larva (Guiney *et al.*, 1997), that the zebrafish larva vasculature is the first site of CYP1A expression. Additionally this expression localizes to one of the first sites of TCDD developmental toxicity, reduced blood flow in the trunk at 72 hpf. Besides the vasculature, the AHR pathway also is activated by TCDD in tissues involved in osmoregulation and circulation, including the gills, kidney, heart, and skin. Whether zfCYP1A is directly involved in TCDD toxicity is unknown. Studies in *O. latipes* and *F. heteroclitus* suggest that TCDD induced apoptosis occurs in the developing vasculature (Cantrell *et al.*, 1998; Toomey *et al.*, 2001) possibly accounting for vascular related signs of toxicity. However this could not be confirmed in rainbow trout larvae (Hornung *et al.*, 1999).

To determine whether zfAHR2 and zfARNT2a/b/c could play a role in TCDD induced zfCYP1A expression, mRNA abundance and tissue specific localization during development was examined. zfAHR2 and zfARNT2a/b/c were both expressed as early as 12 hpf. This precedes the initiation of a beating heart and the first overt signs of TCDD developmental toxicity. This is consistent with results in *F. heteroclitus* where expression of AHR2 and ARNT2 preceded the onset of circulation (Powell *et al.*, 2000). The abundance of zfAHR2 and zfARNT2 mRNAs is relatively constant from 24 to 120 hpf.

Previous studies in rainbow trout and zebrafish cell lines and whole trout and zebrafish demonstrated that AHR2 but not ARNT2 mRNAs could be induced by TCDD-exposure (Abnet *et al.*, 1999; Tanguay *et al.*, 1999). However, it was not known if a lower TCDD-exposure concentration could either increase the abundance or alter the localization of zfAHR2 or zfARNT2a/b/c mRNA. Expression of zfARNT2a/b/c mRNA was not altered by TCDD exposure. However, whole embryonic mRNA abundance of zfAHR2 was marginally, but significantly increased by TCDD at 48 hpf. This was also observed in zebrafish embryos exposed to higher TCDD

concentrations (3.7–30 nM) than used in the present study (1.55 nM) (Tanguay *et al.*, 1999). Since the lower TCDD concentration used in the current investigation was still sufficient to cause 100% mortality and only transiently altered zfAHR2 mRNA abundance it suggests that TCDD developmental toxicity in the zebrafish is not likely dependent on an elevation of whole larva zfAHR2 mRNA expression.

zfAHR2 and zfARNT2b form functional dimeric complexes *in vitro*, but it was unknown whether these 2 proteins would be co-expressed in TCDD responsive tissues. If zfAHR2 and zfARNT2 are essential for TCDD responsiveness *in vivo*, they should be expressed in the same tissues, and should co-localize with TCDD-induced zfCYP1A mRNA and protein expression. zfAHR2, zfARNT2, and TCDD-induced zfCYP1A mRNAs were similarly localized in the vasculature, heart, trunk kidney, ear, and skin by 48 hpf. zfAHR2 and zfARNT2 are presumed to be functional during early development because the TCDD-induced zfCYP1A induction co-localizes with zfAHR2 and zfARNT2 at this time. Confirming the quantitative results, TCDD not only had little effect on whole larval mRNA abundance but localization of zfAHR2 and zfARNT2 were not drastically affected either. Immunohistochemical localization of zfCYP1A suggests that zfAHR2 and zfARNT2a/b/c are responsible for the induction of CYP1A by TCDD as both are co-localized in the vasculature and skin. Identification of the vascular system as a site of zfCYP1A expression is not unique to TCDD-exposed zebrafish larvae. Vascular specific and ligand dependent CYP1A expression has been observed in every fish species studied as well as in the chicken and mouse (Dey *et al.*, 1999; Guiney *et al.*, 1997; Iwata and Stegeman, 2000; Schlezinger and Stegeman, 2000; Smolowitz *et al.*, 1992; Stegeman *et al.*, 1989, 2001; Van Veld *et al.*, 1997; Walker *et al.*, 2000). Expression in the nervous system was similar between zfAHR2 and zfARNT2 in some tissues. zfAHR2 and zfARNT2 were detected in the brain, spinal cord, and sensory organs in the head; however, TCDD-induced zfCYP1A expression was not. The lack of detection of zfCYP1A expression in the head (except for vascular tissues) suggests that zfAHR2 and zfARNT2 most likely have other physiological functions besides altering expression of the TCDD induced battery of genes. A comparison of the localization of AHR, ARNT, and ARNT2 in rat brain suggests that ARNT2 may interact with other PAS proteins (Petersen *et al.*, 2000). The very neuronal specific expression of zfARNT2 as early as 18 hpf in the zebrafish larva brain suggests its involvement in pathways other than AHR signaling as has been postulated in mammals (Michaud *et al.*, 2000).

Comparison of Tissue-Specific Expression of AHR, ARNT, and CYP1A in Zebrafish and Mammals

The expression pattern of AHR in mice and zfAHR2 in zebrafish share some similarities during early development. Initially AHR and zfAHR2 mRNAs are expressed by both

species in neuroepithelia and then expression in this tissue declines with age (Abbott *et al.*, 1995). As the AHR levels decline in nervous system, expression increases in the liver. Although zfAHR2 was not detected in the liver of developing zebrafish, it is expressed in adult liver (Andreassen *et al.*, 2002). The inability to localize zfAHR2 in other tissues of endodermal origin, as has been seen in mice, is probably due to the low sensitivity of the assay and/or the small size of the organs in zebrafish larvae. The expression pattern of zfARNT2a/b/c mRNA in zebrafish larvae differs from mammalian ARNT and ARNT2. In mice ARNT initially is expressed in neuroepithelial tissues and tissues of endodermal and mesodermal origin (Jain *et al.*, 1998). Expression of ARNT2 in the mammalian nervous system declines with age but is still evident in the adult rat brain (Kainu *et al.*, 1995; Petersen *et al.*, 2000). ARNT2 is predominately expressed in the neuroepithelia and only weakly detected in tissues of endodermal and mesodermal origin during development (Jain *et al.*, 1998). The expression pattern of zfARNT2a/b/c is clearly evident in the brain during early development. The pattern of zfARNT2a/b/c mRNA expression thereafter resembles zfARNT2b/c in adult zebrafish where expression predominates in the brain and also in tissues of ectodermal and mesodermal origin such as the eye, gill, muscle, and skin with very little expression in the kidney, heart, and liver (Tanguay *et al.*, 2000). However, zfARNT2, unlike mammalian ARNT or ARNT2, is evident in tissues of ectodermal origin in the zebrafish larvae. Expression of CYP1A1 mRNA in mammals is somewhat similar to zebrafish. In mice exposure to the AHR agonist 3-methylcholanthrene was necessary to detect CYP1A by *in situ* analysis. Following 3-methylcholanthrene treatment of 5- to 6-week-old mice, CYP1A was detected in mice in the liver, brain (especially endothelial cells lining the choroid plexus, cerebrum, and cerebellum), gastrointestinal tract, and the endothelium of blood vessels throughout the body (Dey *et al.*, 1999). A similar pattern of expression is observed in zebrafish larvae exposed to TCDD.

Colocalization of zfAHR2, zfARNT2, and zfCYP1A mRNAs during Zebrafish Development

Some interesting effects of TCDD exposure on mRNA expression in zebrafish larvae were observed. In mesoderm-derived tissues zfAHR2, zfARNT2a/b/c, and TCDD-induced zfCYP1A mRNA expression were similarly localized in the vasculature, heart, and trunk kidney by 48 hpf. zfAHR2 and zfARNT2a/b/c were expressed in the mesenchyme in the head but TCDD induced zfCYP1A was not detected in these tissues. TCDD induced zfCYP1A was detected in hematopoietic tissues and renal tubules, however, zfAHR2 and zfARNT2a/b/c were not seen in these tissues. Comparisons of ectodermal expression revealed that zfAHR2 and zfARNT2a/b/c were detected in the brain, spinal cord, and sensory organs. However, TCDD induced zfCYP1A expression was not detected in these tissues. zfAHR2, zfARNT2a/b/c, and TCDD induced

zfCYP1A were all colocalized in the ear and skin. In endoderm-derived tissues, all 3 mRNAs were detected in the oropharyngeal mucosa and intestinal mucosa by 120 hpf.

The lack of TCDD induced zfCYP1A expression in tissues expressing zfAHR2 and zfARNT2a/b/c may be accounted for in several ways. Perhaps an AHR repressor (AHRR) or other factors inhibit zfAHR2 activity. The zfARNT2 detected in these tissues may be predominately composed of the splice variants that are not active with zfAHR2 namely zfARNT2a/c. The TCDD induced expression zfCYP1A in tissues devoid of zfAHR2 and zfARNT2 may be due to insufficient sensitivity of the detection method or perhaps another uncharacterized AHR or ARNT regulates zfCYP1A expression in these tissues.

The tissue-specific expression of zfAHR2, zfARNT2a/b/c, and zfCYP1A characterized in zebrafish embryos and larvae exposed to vehicle (control) or TCDD supports the hypothesis that the AHR is involved in TCDD developmental toxicity. This is evidenced by the expression of zfAHR2 and zfARNT2a/b/c preceding the onset of the first signs of TCDD developmental toxicity. Additionally increased expression of zfCYP1A in TCDD target tissues colocalizes with zfAHR2 and zfARNT2a/b/c. The abundance and localization of the messages of these 2 transcription factors was not drastically affected by embryonic TCDD exposure implying that altered expression of these genes is not involved in TCDD toxicity. TCDD induced zfCYP1A protein and mRNA expression in the cardiovascular system and tissues involved in osmoregulation suggest that the AHR is activated by TCDD in those larval tissues involved in TCDD developmental toxicity. Additionally colocalization of zfAHR2 and zfARNT2a/b/c in these tissues is consistent with the well known involvement of AHR and ARNT proteins in the TCDD dependent induction of CYP1A1 in mammalian model systems.

The expression of both zfAHR2 and zfARNT2a/b/c in the central nervous system suggests that they may have functional roles in nervous system development and/or function. The AHR pathway is active in early vascular development and in tissues involved in osmoregulation following TCDD exposure. Taken together, these findings implicate the cardiovascular, osmoregulatory, and central nervous systems as key sites of action of TCDD in causing developmental toxicity in zebrafish. The effect of TCDD on these organ systems at the cellular and molecular level during zebrafish larval development is the focus of future work.

ACKNOWLEDGMENTS

We thank Dorothy Nesbit for her excellent technical support and Amanda Laughlin for her help with the immunofluorescence technique. This work was supported in part by NIEHS grant ES10820 (R.L.T.), the NIEHS Developmental and Molecular Toxicology Center Grant P30ES09090 (W.H. and R.E.P.), and the University of Wisconsin Sea Grant Institute under grants from the National Sea Grant College Program, National Oceanic and Atmospheric Administration, US Department of Commerce, Sea Grant Project Numbers R/BT12 and R/BT14 (W.H. and R.E.P.). Additional support was provided by

Oregon State University Marine/Freshwater Biomedical Science Center (NIEHS grant ES03850).

REFERENCES

- Abbott, B. D., Birnbaum, L. S., and Perdew, G. H. (1995). Developmental expression of two members of a new class of transcription factors: I. Expression of aryl hydrocarbon receptor in the C57BL/6N mouse embryo. *Dev. Dyn.* **204**, 133–143.
- Abnet, C. C., Tanguay, R. L., Hahn, M. E., Heideman, W., and Peterson, R. E. (1999). Two forms of aryl hydrocarbon receptor type 2 in rainbow trout (*Oncorhynchus mykiss*). Evidence for differential expression and enhancer specificity. *J. Biol. Chem.* **274**, 15159–15166.
- Andreasen, E. A., Hahn, M. E., Heideman, W., Peterson, R. E., and Tanguay, R. L. (2002). The zebrafish (*Danio rerio*) aryl hydrocarbon receptor type 1 (zfAHR1) is a novel vertebrate receptor. *Mol. Pharmacol.* **62**, 234–249.
- Belair, C. D., Peterson, R. E., and Heideman, W. (2001). Disruption of erythropoiesis by dioxin in the zebrafish. *Dev. Dyn.* **222**, 581–594.
- Binder, R. L., and Stegeman, J. J. (1984). Microsomal electron transport and xenobiotic monooxygenase activities during the embryonic period of development in the killifish, *Fundulus heteroclitus*. *Toxicol. Appl. Pharmacol.* **73**, 432–443.
- Binder, R. L., Stegeman, J. J., and Lech, J. J. (1985). Induction of cytochrome P-450-dependent monooxygenase systems in embryos and eleutheroembryos of the killifish *Fundulus heteroclitus*. *Chem. Biol. Interact.* **55**, 185–202.
- Buchmann, A., Wannemacher, R., Kulzer, E., Buhler, D. R., and Bock, K. W. (1993). Immunohistochemical localization of the cytochrome P450 isozymes LMC2 and LM4B (P4501A1) in 2,3,7,8-tetrachlorodibenzo-*p*-dioxin-treated zebrafish (*Brachydanio rerio*). *Toxicol. Appl. Pharmacol.* **123**, 160–169.
- Cantrell, S. M., Joy-Schleizinger, J., Stegeman, J. J., Tillitt, D. E., and Hannink, M. (1998). Correlation of 2,3,7,8-tetrachlorodibenzo-*p*-dioxin-induced apoptotic cell death in the embryonic vasculature with embryotoxicity. *Toxicol. Appl. Pharmacol.* **148**, 24–34.
- Dey, A., Jones, J. E., and Nebert, D. W. (1999). Tissue- and cell type-specific expression of cytochrome P450 1A1 and cytochrome P450 1A2 mRNA in the mouse localized by *in situ* hybridization. *Biochem. Pharmacol.* **58**, 525–537.
- Elonen, G. E., Spehar, R. L., Holcombe, G. W., Johnson, R. D., Fernandez, J. D., Erickson, R. J., Tietge, J. E., and Cook, P. M. (1998). Comparative toxicity of 2,3,7,8-tetrachlorodibenzo-*p*-dioxin to seven freshwater fish species during early life-stage development. *Environ. Toxicol. Chem.* **17**, 472–483.
- Fernandez-Salguero, P. M., Hilbert, D. M., Rudikoff, S., Ward, J. M., and Gonzalez, F. J. (1996). Aryl-hydrocarbon receptor-deficient mice are resistant to 2,3,7,8-tetrachlorodibenzo-*p*-dioxin-induced toxicity. *Toxicol. Appl. Pharmacol.* **140**, 173–179.
- Guiney, P. D., Smolowitz, R. M., Peterson, R. E., and Stegeman, J. J. (1997). Correlation of 2,3,7,8-tetrachlorodibenzo-*p*-dioxin induction of cytochrome P4501A in vascular endothelium with toxicity in early life stages of lake trout. *Toxicol. Appl. Pharmacol.* **143**, 256–273.
- Guiney, P. D., Walker, M. K., Spitsbergen, J. M., and Peterson, R. E. (2000). Hemodynamic dysfunction and cytochrome P4501A mRNA expression induced by 2,3,7,8-tetrachlorodibenzo-*p*-dioxin during embryonic stages of lake trout development. *Toxicol. Appl. Pharmacol.* **168**, 1–14.
- Hahn, M. E., Karchner, S. I., Shapiro, M. A., and Perera, S. A. (1997). Molecular evolution of two vertebrate aryl hydrocarbon (dioxin) receptors (AHR1 and AHR2) and the PAS family. *Proc. Natl. Acad. Sci. U.S.A.* **94**, 13743–13748.
- Henry, T. R., Spitsbergen, J. M., Hornung, M. W., Abnet, C. C., and Peterson, R. E. (1997). Early life stage toxicity of 2,3,7,8-tetrachlorodibenzo-*p*-dioxin in zebrafish (*Danio rerio*). *Toxicol. Appl. Pharmacol.* **142**, 56–68.
- Hornung, M. W., Spitsbergen, J. M., and Peterson, R. E. (1999). 2,3,7,8-Tetrachlorodibenzo-*p*-dioxin alters cardiovascular and craniofacial development and function in sac fry of rainbow trout (*Oncorhynchus mykiss*). *Toxicol. Sci.* **47**, 40–51.
- Hosoya, T., Oda, Y., Takahashi, S., Morita, M., Kawauchi, S., Ema, M., Yamamoto, M., and Fujii-Kuriyama, Y. (2001). Defective development of secretory neurones in the hypothalamus of Arnt2-knockout mice. *Genes Cells* **6**, 361–374.
- Hsu, H. J., Wang, W. D., and Hu, C. H. (2001). Ectopic expression of negative ARNT2 factor disrupts fish development. *Biochem. Biophys. Res. Commun.* **282**, 487–492.
- Husoy, A. M., Myers, M. S., Willis, M. L., Collier, T. K., Celander, M., and Goksoyr, A. (1994). Immunohistochemical localization of CYP1A and CYP3A-like isozymes in hepatic and extrahepatic tissues of Atlantic cod (*Gadus morhua* L.), a marine fish. *Toxicol. Appl. Pharmacol.* **129**, 294–308.
- Iwata, H., and Stegeman, J. J. (2000). *In situ* RT-PCR detection of CYP1A mRNA in pharyngeal epithelium and chondroid cells from chemically untreated fish: Involvement in vertebrate craniofacial skeletal development? *Biochem. Biophys. Res. Commun.* **271**, 130–137.
- Jain, S., Maltepe, E., Lu, M. M., Simon, C., and Bradfield, C. A. (1998). Expression of ARNT, ARNT2, HIF1 α , HIF2 α and Ah receptor mRNAs in the developing mouse. *Mech. Dev.* **73**, 117–123.
- Johnson, R. D., Tietge, J. E., Jensen, K. M., Fernandez, J. D., Linnum, A. L., Lothenbach, D. B., Holcombe, G. W., Cook, P. M., Christ, S. A., Lattier, D. L., and Gordon, D. A. (1998). Toxicity of 2,3,7,8-tetrachlorodibenzo-*p*-dioxin to early life stage brook trout (*Salvelinus fontinalis*) following parental dietary exposure. *Environ. Toxicol. Chem.* **17**, 2408–2411.
- Kainu, T., Gustafsson, J. A., and Pelto-Huikko, M. (1995). The dioxin receptor and its nuclear translocator (Arnt) in the rat brain. *Neuroreport* **6**, 2557–2560.
- Lahvis, G. P., Lindell, S. L., Thomas, R. S., McCuskey, R. S., Murphy, C., Glover, E., Bentz, M., Southard, J., and Bradfield, C. A. (2000). Portosystemic shunting and persistent fetal vascular structures in aryl hydrocarbon receptor-deficient mice. *Proc. Natl. Acad. Sci. U.S.A.* **97**, 10442–10447.
- Mattingly, C. J., and Toscano, W. A. (2001). Posttranscriptional silencing of cytochrome P4501A1 (CYP1A1) during zebrafish (*Danio rerio*) development. *Dev. Dyn.* **222**, 645–654.
- Michaud, J. L., DeRossi, C., May, N. R., Holdener, B. C., and Fan, C. M. (2000). ARNT2 acts as the dimerization partner of SIM1 for the development of the hypothalamus. *Mech. Dev.* **90**, 253–261.
- Mimura, J., Yamashita, K., Nakamura, K., Morita, M., Takagi, T. N., Nakao, K., Ema, M., Sogawa, K., Yasuda, M., Katsuki, M., and Fujii-Kuriyama, Y. (1997). Loss of teratogenic response to 2,3,7,8-tetrachlorodibenzo-*p*-dioxin (TCDD) in mice lacking the Ah (dioxin) receptor. *Genes Cells* **2**, 645–654.
- Park, S. S., Miller, H., Klotz, A. V., Kloepper-Sams, P. J., Stegeman, J. J., and Gelboin, H. V. (1986). Monoclonal antibodies to liver microsomal cytochrome P-450E of the marine fish *Stenotomus chrysops* (scup): Cross reactivity with 3-methylcholanthrene induced rat cytochrome P-450. *Arch. Biochem. Biophys.* **249**, 339–350.
- Peters, J. M., Narotsky, M. G., Elizondo, G., Fernandez-Salguero, P. M., Gonzalez, F. J., and Abbott, B. D. (1999). Amelioration of TCDD-induced teratogenesis in aryl hydrocarbon receptor (AhR)-null mice. *Toxicol. Sci.* **47**, 86–92.
- Petersen, S. L., Curran, M. A., Marconi, S. A., Carpenter, C. D., Lubbers, L. S., and McAbee, M. D. (2000). Distribution of mRNAs encoding the arylhydrocarbon receptor, arylhydrocarbon receptor nuclear translocator, and arylhydrocarbon receptor nuclear translocator-2 in the rat brain and brainstem. *J. Comp. Neurol.* **427**, 428–439.
- Pollenz, R. S., Sullivan, H. R., Holmes, J., Necela, B., and Peterson, R. E. (1996). Isolation and expression of cDNAs from rainbow trout (*Oncorhynchus mykiss*) that encode two novel basic helix-loop-Helix/PER-ARNT-SIM

- (bHLH/PAS) proteins with distinct functions in the presence of the aryl hydrocarbon receptor. Evidence for alternative mRNA splicing and dominant negative activity in the bHLH/PAS family. *J. Biol. Chem.* **271**, 30886–30896.
- Powell, W. H., Bright, R., Bello, S. M., and Hahn, M. E. (2000). Developmental and tissue-specific expression of AHR1, AHR2, and ARNT2 in dioxin-sensitive and -resistant populations of the marine fish *Fundulus heteroclitus*. *Toxicol. Sci.* **57**, 229–239.
- Powell, W. H., and Hahn, M. E. (2000). The evolution of aryl hydrocarbon signaling proteins: Diversity of ARNT isoforms among fish species. *Mar. Environ. Res.* **50**, 39–44.
- Rowlands, J. C., and Gustafsson, J. A. (1997). Aryl hydrocarbon receptor-mediated signal transduction. *Crit. Rev. Toxicol.* **27**, 109–134.
- Schleizinger, J. J., and Stegeman, J. J. (2000). Dose and inducer-dependent induction of cytochrome P450 1A in endothelia of the eel, including in the swimbladder rete mirabile, a model microvascular structure. *Drug Metab. Dispos.* **28**, 701–708.
- Schmidt, J. V., and Bradfield, C. A. (1996). Ah receptor signaling pathways. *Annu. Rev. Cell Dev. Biol.* **12**, 55–89.
- Schmidt, J. V., Su, G. H., Reddy, J. K., Simon, M. C., and Bradfield, C. A. (1996). Characterization of a murine Ahr null allele: Involvement of the Ah receptor in hepatic growth and development. *Proc. Natl. Acad. Sci. U.S.A.* **93**, 6731–6736.
- Smolowitz, R. M., Hahn, M. E., and Stegeman, J. J. (1991). Immunohistochemical localization of cytochrome P-450IA1 induced by 3,3',4,4'-tetrachlorobiphenyl and by 2,3,7,8-tetrachlorodibenzoafuran in liver and extrahepatic tissues of the teleost *Stenotomus chrysops* (scup). *Drug Metab. Dispos.* **19**, 113–123.
- Smolowitz, R. M., Schultz, M. E., and Stegeman, J. J. (1992). Cytochrome P450IA induction in tissues, including olfactory epithelium, of topminnows (*Poeciliopsis* spp.) by waterborne benzo[a]pyrene. *Carcinogenesis* **13**, 2395–2402.
- Spitsbergen, J. M., Walker, M. K., Olson, J. R., and Peterson, R. E. (1990). Pathologic alterations in early life stages of lake trout, *Salvelinus namaycush*, exposed to 2,3,7,8-tetrachlorodibenzo-*p*-dioxin as fertilized eggs. *Aquat. Toxicol.* **19**, 41–72.
- Stegeman, J. J., Miller, M. R., and Hinton, D. E. (1989). Cytochrome P450IA1 induction and localization in endothelium of vertebrate (teleost) heart. *Mol. Pharmacol.* **36**, 723–729.
- Stegeman, J. J., Schleizinger, J. J., Craddock, J. E., and Tillitt, D. E. (2001). Cytochrome P450 1A expression in midwater fishes: Potential effects of chemical contaminants in remote oceanic zones. *Environ. Sci. Technol.* **35**, 54–62.
- Sutter, T. R., and Greenlee, W. F. (1992). Classification of members of the Ah gene battery. *Chemosphere* **25**, 223–226.
- Sutter, T. R., Guzman, K., Dold, K. M., and Greenlee, W. F. (1991). Targets for dioxin: Genes for plasminogen activator inhibitor-2 and interleukin-1 β . *Science* **254**, 415–418.
- Tanguay, R. L., Abnet, C. C., Heideman, W., and Peterson, R. E. (1999). Cloning and characterization of the zebrafish (*Danio rerio*) aryl hydrocarbon receptor. *Biochim. Biophys. Acta* **1444**, 35–48.
- Tanguay, R. L., Andreasen, E., Heideman, W., and Peterson, R. E. (2000). Identification and expression of alternatively spliced aryl hydrocarbon nuclear translocator 2 (ARNT2) cDNAs from zebrafish with distinct functions. *Biochim. Biophys. Acta* **1494**, 117–128.
- Teraoka, H., Dong, W., Ogawa, S., Tsukiyama, S., Okuhara, Y., Niiyama, M., Ueno, N., Peterson, R. E., and Hiraga, T. (2002). 2,3,7,8-Tetrachlorodibenzo-*p*-dioxin toxicity in the zebrafish embryo: Altered regional blood flow and impaired lower jaw development. *Toxicol. Sci.* **65**, 192–199.
- Toomey, B. H., Bello, S., Hahn, M. E., Cantrell, S., Wright, P., Tillitt, D. E., and Di Giulio, R. T. (2001). 2,3,7,8-Tetrachlorodibenzo-*p*-dioxin induces apoptotic cell death and cytochrome P4501A expression in developing *Fundulus heteroclitus* embryos. *Aquat. Toxicol.* **53**, 127–38.
- Van Veld, P. A., Vogelbein, W. K., Cochran, M. K., Goksoyr, A., and Stegeman, J. J. (1997). Route-specific cellular expression of cytochrome P4501A (CYP1A) in fish (*Fundulus heteroclitus*) following exposure to aqueous and dietary benzo[a]pyrene. *Toxicol. Appl. Pharmacol.* **142**, 348–359.
- Walker, M. K., Heid, S. E., Smith, S. M., and Swanson, H. I. (2000). Molecular characterization and developmental expression of the aryl hydrocarbon receptor from the chick embryo. *Comp. Biochem. Physiol. C Toxicol. Pharmacol.* **126**, 305–319.
- Walker, M. K., and Peterson, R. E. (1991). Potencies of polychlorinated dibenzo-*p*-dioxin, dibenzofuran and biphenyl congeners, relative to 2,3,7,8-tetrachlorodibenzo-*p*-dioxin, for producing early life stage mortality in rainbow trout (*Oncorhynchus mykiss*). *Aquat. Toxicol.* **21**, 219–237.
- Walker, M. K., and Peterson, R. E. (1994). Aquatic toxicity of dioxins and related chemicals. In *Dioxins and Health* (A. Schecter, Ed.), pp. 347–387. Plenum Press, New York.
- Walker, M. K., Spitsbergen, J. M., Olson, J. R., and Peterson, R. E. (1991). 2,3,7,8-Tetrachlorodibenzo-*p*-dioxin (TCDD) toxicity during early life stage development of lake trout (*Salvelinus namaycush*). *Can. J. Fish Aquat. Sci.* **48**, 875–883.
- Wang, W. D., Chen, Y. M., and Hu, C. H. (1998). Detection of Ah receptor and Ah receptor nuclear translocator mRNAs in the oocytes and developing embryos of zebrafish (*Danio rerio*). *Fish Physiol. Biochem.* **18**, 49–57.
- Westerfield, M. (1995). *The Zebrafish Book*. University of Oregon Press, Eugene, OR.
- Zabel, E. W., Cook, P. M., and Peterson, R. E. (1995). Toxic equivalency factors of polychlorinated dibenzo-*p*-dioxin, dibenzofuran and biphenyl congeners based on early life stage mortality in rainbow trout (*Oncorhynchus mykiss*). *Aquat. Toxicol.* **31**, 315–328.
- Zabel, E. W., Pollenz, R., and Peterson, R. E. (1996). Relative potencies of individual polychlorinated dibenzo-*p*-dioxin, dibenzofuran, and biphenyl congeners and congener mixtures based on induction of cytochrome P4501A mRNA in a rainbow trout gonadal cell line (RTG-2). *Environ. Toxicol. Chem.* **15**, 2310–2318.